

CHARACTERIZATION OF ASPHALT/RECYCLED PLASTIC BLENDS MODIFIED BY  
EXFOLIATED CLAY NANOPATELETS

By

Kate A. Nguyen

Presented to the Faculty of the Graduate School of  
The University of Texas at Arlington in Partial Fulfillment  
of the Requirements for the Degree of

MASTER OF SCIENCE IN MATERIALS SCIENCE AND ENGINEERING

THE UNIVERSITY OF TEXAS AT ARLINGTON

May 2021

Copyright © by Kate A. Nguyen 2021

All Rights Reserved

## **ACKNOWLEDGEMENTS**

I would like to thank my advisor, Dr. Maria S. Konsta-Gdoutos, for her confidence and support in my graduate studies. I would like to extend my gratitude to Dr. Panagiotis Danoglidis for his knowledge and enthusiasm in research. Also, to my lab members, Myrsini Maglogianni and Michail Margas, for their help and camaraderie through the pandemic. Their guidance was invaluable to me as I progressed in a new field of study.

Thank you to my committee members, Dr. Efstathios I. Meletis and Dr. Erika La Plante, for their time and feedback in reviewing my thesis defense. I am grateful to have been a part of the Center for Advanced Construction Materials.

Lastly, my greatest appreciation to family and friends who have encouraged me in life and academia. I am forever thankful to my husband W. Chris Reddig for being my believer, constant motivator, and emotional support.

May 4, 2021

## **ABSTRACT**

### **CHARACTERIZATION OF ASPHALT/RECYCLED PLASTIC BLENDS MODIFIED BY EXFOLIATED CLAY NANOPATELETS**

Kate A. Nguyen, MS

The University of Texas at Arlington, 2021

Supervising Professor: Maria S. Konsta-Gdoutos

There is a renewed interest from federal and state transportation agencies as well as the asphalt industry in developing successful utilization of recycled plastics in asphalt pavements. By incorporating a third material into the asphalt/plastic blend, a stimulation of enhanced compatibility between the waste plastics and asphalt can be observed. In this thesis, the need for increased stability and improved mechanical performance of asphalt blends, at low and high temperatures, are addressed through the use of dispersed/exfoliated organic montmorillonite nanoplatelets a.k.a. nanoclay (NC). Previous studies with non-dispersed NC as a modifier in asphalt (AS) and polyethylene (PE) blends reported the addition of NC may have the potential to modify the natural viscoelastic behavior, thus affecting the thermal stability.

This project aims to introduce an innovative technology for the production of a novel asphalt blend that is an environmentally friendly, viable, and more economical alternative for pavement construction. The stability and enhanced cracking/rutting

resistance at cold and hot temperatures of the product will contribute to improving the safety and serviceability of roadways while reducing the maintenance/repair costs.

Fourier-transform infrared (FTIR) spectroscopy analyses conducted showed evidence of new chemical interactions between the dispersed nanoparticles and asphalt/plastic blend, suggesting a better-blended phase morphology. The indirect tensile (IDT) strength test was performed on AS/PE blends with and without reinforced NC, both dispersed and non-dispersed. The results showed an increase in tensile strength and the stress-strain ratio of the proposed material that indicates a higher modulus of elasticity. Scanning electron microscopy (SEM) was also used to examine the fracture surface of the AS/PE/NC-d sample to identify the presence of NC.

## TABLE OF CONTENTS

ACKNOWLEDGEMENTS .....	ii
ABSTRACT .....	1
LIST OF FIGURES.....	5
LIST OF TABLES.....	6
CHAPTER 1 .....	7
CHAPTER 2 .....	9
2.1 Asphalt Concrete.....	9
2.1.1 Fatigue Cracking and Rutting.....	9
2.1.2 Modification with Waste Plastics .....	11
2.1.3 Incorporation of Montmorillonite .....	12
2.2 Performance Testing and Analysis of Asphalt Specimens .....	14
2.2.1 Fourier Transform Infrared Spectroscopy.....	14
2.2.2 Indirect Tensile Test.....	16
2.2.3 Scanning Electron Microscopy .....	17
CHAPTER 3 .....	20
3.1 Experimental Procedure.....	20
3.1.1 Dispersion of Nanoplatelets .....	21
3.1.2 Preparation of Modified Asphalt Specimens.....	21
3.2 FTIR Characterization .....	23
3.3 IDT Testing.....	24
3.4 SEM Analysis .....	25

CHAPTER 4 .....	26
4.1 FTIR Characterization .....	26
4.2 Stress-Strain Behavior of Asphalt Blends.....	30
4.3 Fracture Surface Imaging.....	32
CHAPTER 5 .....	36
5.1 Conclusions.....	36
5.2 Future research.....	36

## LIST OF FIGURES

Figure 2.1 Severely fatigued cracked pavement [12] .....	10
Figure 2.2 Severe mix rutting [15] .....	10
Figure 2.3 Model diagram of montmorillonite clay structure [27] .....	13
Figure 2.4 Schematic of structures of layered silicate modified asphalts [30] .....	14
Figure 2.5 Thermo Nicolet iS50 FTIR Spectrometer .....	15
Figure 2.6 Schematic of an interferometer [33] .....	16
Figure 2.7 IDT sample schematic [38].....	17
Figure 2.8 Schematic diagram of a SEM [39].....	18
Figure 2.9 Illustration of signals generated from electron-specimen interactions [39] ...	19
Figure 3.1 Graduation curves of fine and coarse aggregates.....	21
Figure 3.2 EIRICH Intensive Mixer Type RV02E.....	23
Figure 3.3 Top and side view of the AS/PE sample .....	23
Figure 3.4 IDT strength test of the AS/PE sample.....	24
Figure 3.5 HITACHI S-3000N SEM.....	25
Figure 4.1 FTIR spectra of dispersed vs. non-dispersed nanoclay .....	28
Figure 4.2 FTIR spectra of PG 64-22 asphalt, polyethylene, and nanoclay .....	29
Figure 4.3 FTIR spectra of asphalt blends .....	30
Figure 4.4 Stress-strain curve of IDT testing of the specimens .....	31
Figure 4.5 BSE-SEM image of AS/PE/NC-d at 450x magnification.....	33
Figure 4.6 BSE-SEM image of AS/PE/NC-d at 1800x magnification.....	33
Figure 4.7 EDS spectra of spot analyses .....	34
Figure 4.8 Element composition mapping at 1800x magnification .....	35



## LIST OF TABLES

Table 3.1 Properties of nanoclay particles (NC).....	20
Table 3.2 Composition of modified asphalt specimens by weight percent .....	22
Table 4.1 Indirect tensile strength of the specimens .....	32
Table 4.2 Atom percent of spots at 1800x magnification.....	35

# CHAPTER 1

## INTRODUCTION

Asphalt has been primarily used in road construction as a binder. It is obtained as petroleum distillate residues with strong adhesion and hydrophobic properties. However, there are limits to the serviceability of asphalt pavements due to failures, such as high-temperature rutting or low-temperature cracking, and require further modifications. Waste plastics were considered as a modifier from the environmental and economic benefits of repurposing recycled materials. The results from these studies report some improved parameters, such as thermal stability and fatigue behavior, but also show negative effects on material properties depending on the type of plastic used [1-4].

Recently, there has been a re-established interest by the U.S. Department of Transportation and the Federal Highway Administration (FHWA) in domestic pavement applications using recycled plastics to enhance the mechanical properties of asphalt blends and address the environmental impacts of production and installation. Among the benefits of reducing the amount of single-use waste plastic in landfills, the application of recycled plastic in pavements can reduce carbon emission and material costs without expending additional energy [5]. Field projects have begun to validate the long-term performance in various countries including India, New Zealand, and South Africa [6-8].

For improved serviceability and operation efficiency, new studies were completed for the enhanced compatibility between asphalt and plastic utilizing various methods. In 2020, the FHWA the Exploratory Advanced Research Program No. 693JJ3-20-BAA-

0001 for research proposals to advance highway engineering and intermodal surface transportation in the United States. Specifically, Topic 3 addresses the need for compatibilization by addition of a third material. In this research, we investigated a novel technique of incorporating dispersed/exfoliated organic montmorillonite nanoplatelets, or nanoclay. Compared to prior research on this third material, this new approach can further develop the mechanical performance of asphalt blends.

In the following chapters, the technology developed for modified asphalt and analyses are reviewed in chapter 2. The methodology and experimental procedure are detailed in chapter 3, followed by the results discussed in chapter 4. Finally, the conclusion is summarized, and future developments are explained in chapter 5.

## **CHAPTER 2**

### **BACKGROUND**

#### **2.1 Asphalt Concrete**

Asphalt concrete, or asphalt pavement, is a composite of aggregates bound with asphalt (AS). Performance graded (PG) asphalt binders are developed with Superpave specifications to resist high-temperature rutting, fatigue cracking, and low-temperature cracking. The grade designations are labels based on the average 7-day maximum pavement temperature and the minimum pavement temperature (°C). In Texas, the asphalt binder grade PG 64-22 is commonly used based on the climate parameters [9]. Even with upgraded asphalt binders, weather events like Winter Storm Uri in February 2021 can exacerbate deformation brought on by the unprecedented low temperatures.

##### ***2.1.1 Fatigue Cracking and Rutting***

The most common distresses in asphalt pavement are classified as fatigue cracking and permanent deformation (rutting). The factors that affect these distresses are categorized into three groups: material properties, environmental and traffic conditions, and construction quality [10,11].

After repeating loading, pavements are susceptible to fatigue cracking, illustrated in Figure 2.1. This appears as a series of interconnected crack lines that expand rapidly and exponentially [12]. In thin pavements, classical (bottom-up) cracking occurs in which cracks are initiated from the bottom layer of asphalt where tensile stresses are greater and propagate upwards. Conversely, thicker pavements observe a top-down cracking phenomenon due to large localized tensile stresses from contact pressure

between tires and the pavement [12,13]. Attributed to asphalt's flexibility, rutting appears as depressions in the wheel paths [11, 14]. This deformation, exhibited in Figure 2.2, is commonly a result of shear stress from the poor structural design of subgrade layers, lack of compaction, or improper mix design [15].

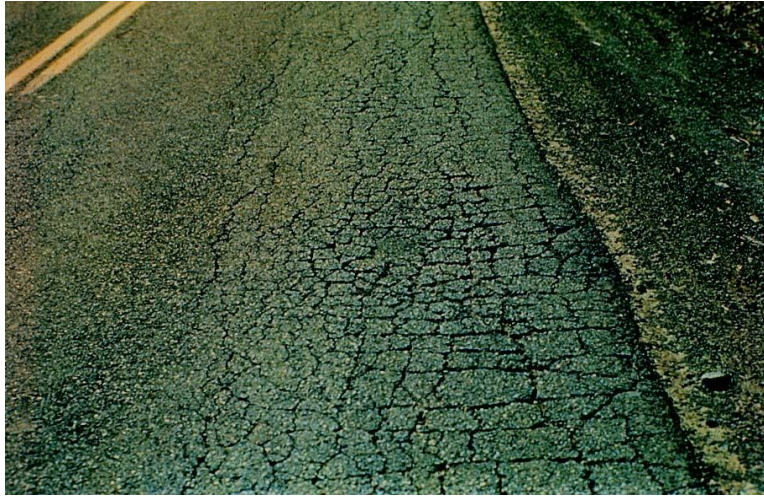


Figure 2.1 Severely fatigued cracked pavement [12]



Figure 2.2 Severe mix rutting [15]

### **2.1.2 Modification with Waste Plastics**

Polymers have been introduced as a modifier to improve the mechanical performance of asphalt. The asphalt industry and scientific community have focused on utilizing waste plastics due to the high availability and low cost. Although recent field projects implementing the asphalt/waste plastic blends have been conducted around the world, analyses for long-term performance have not been validated. Additionally, prior research has shown different results depending on the polymer used, the process method, and the parameters measured [4].

As one of the main sources of waste plastics, polyethylene (PE) is commonly used as an asphalt modifier. According to Fang et. al. [1], the addition of waste PE has been shown to improve the properties of asphalt at high and low temperatures. Yet, the low-temperature performance and compatibility of PE-modified asphalt require further development [2]. Enhancing the compatibilization between asphalt and waste plastic is another major technical concern. The lack of integration of these materials can lead to undesirable mechanical properties [16].

There have already been PE modified asphalts developed and commercialized such as Novaphalt and Polyphalt. However, field performances have resulted in the segregation of the plastic and asphalt, low stiffness, and decrease fatigue cracking and rutting resistance. The high shear method required for mixing also lead to undesirable economic return with the use of excessive energy. For instance, the production of Novaphalt was estimated at \$250/ton in comparison to \$25/ton for the manufacture of regular asphalt [17].

Over the years, solutions with the inclusion of aromatic oil-based additives to bolster the compatibility have been suggested and patented. However, the required amount of oil to achieve good compatibility (up to 66 wt%) lead to excessive softening and significant rutting of the asphalt mixtures [18,19]. Other methods based on the formation of covalent bonds between the asphalt and polymer have been investigated, including vulcanization, inactivating polar functionality, Friedel-Crafts reaction, aminolysis, and incorporating nanomaterials [20-25].

### **2.1.3 Incorporation of Montmorillonite**

Nanoparticles have been a new frontier of development with numerous applications in a wide variety of fields. One of the most frequent nanomaterials used for modified asphalt is montmorillonite nanoclay (NC) [26]. This nanoplatelet contains a layered structure with two silica tetrahedrons sandwiching an alumina octahedron, shown in Figure 2.3. NC has been documented to significantly improve the mechanical, thermal, and barrier properties of polymer composites due to its high aspect ratio, large surface area, multiscale structure, and low cost [28,29].

The incorporation of NC has been studied in polymer and asphalt composites individually. Similar to PE/NC blends, the AS/NC structure has two types: intercalated and exfoliated as illustrated in Figure 2.4. The exfoliation has been suggested to increase interactions of the NC in the blends as the layers themselves are intercalated within the matrix. This enhances the improvements compared to the base media.

Zhu et. al. [28] reviewed the latest exfoliation methods of NC in polymer nanocomposites; many studies proved advantageous in improving the properties. Yu et.

al. [30] determined the addition of NC into asphalt increased the viscoelastic properties. You et. al. [26] also concluded the NC-altered asphalt improved the mechanical properties. Fang et. al. [29] demonstrated the effects of combining both PE and NC to asphalt. There were indications of exfoliation of NC during the preparation of the specimens that resulted in asphalt mixtures with excellent deformation resistance, high-temperature stability, and low-temperature anti-cracking performance.

However, effective exfoliation of nanoclay to individual layers into the matrix remains a challenge [28]. In this research, a dispersion method of sonication adopted by Daniel et. al. [31] is proposed for the exfoliation of NC prior to mixing the asphalt blend. This technique has been confirmed to significantly improve the dispersion of nanoclay particles in any matrix.

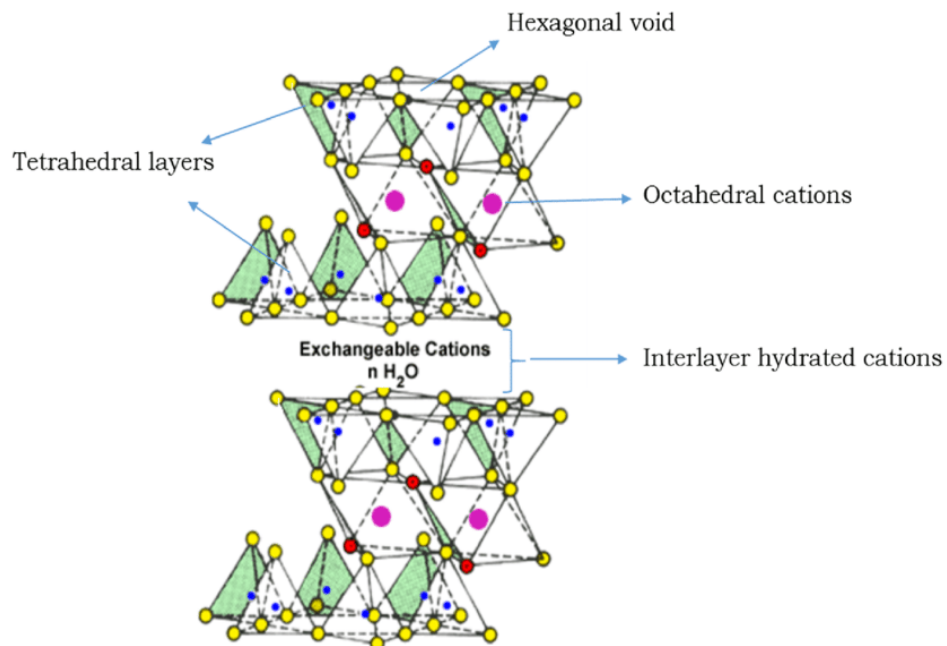


Figure 2.3 Model diagram of montmorillonite clay structure [27]



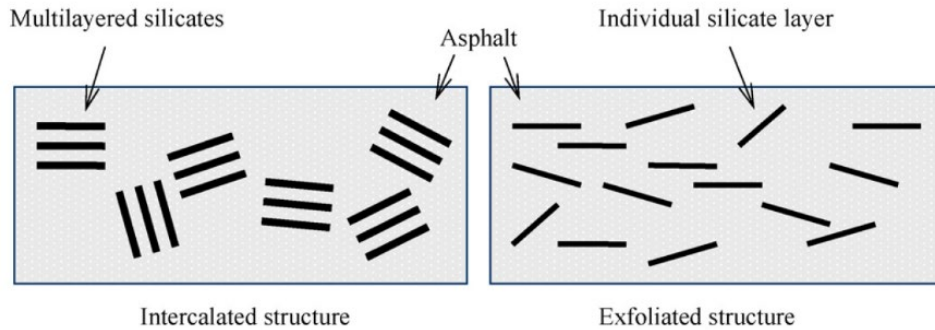


Figure 2.4 Schematic of structures of layered silicate modified asphalts [30]

## 2.2 Performance Testing and Analysis of Asphalt Specimens

Upon reviewing various indicators and testing methods of modified asphalt, Du et. al. [32] recommended that a new, rational, evaluation index is necessary for better characterization. In this section, a brief background on the selected analyses in this research will be given.

### 2.2.1 Fourier Transform Infrared Spectroscopy

Fourier transform infrared (FTIR) spectroscopy is a third-generation technique for material analysis based on the absorption of infrared radiation. The principles of this technique have been established in the past century but only in recent years has it been extensively developed with the advent of high-speed digital computers [33]. Compared to dispersive infrared spectrometers, FTIR provides significant advantages and is the preferred method of spectral analysis. Shown in Figure 2.5, this non-destructive instrument includes improvements such as faster analysis speed and increased sensitivity (Fellgett and Jacquinot Advantages, respectively), mechanical simplicity, and

precise measurements without external calibration (Connes Advantage) with greater optical throughput [34].

An interferometer is utilized instead of a grating monochromator to acquire a spectrum. This mechanism is based on splitting a beam containing all IR wavelengths, with one path at a fixed length and the other of variable length by use of a movable mirror. The differing distances between the split beams yield a sequence of constructive and destructive interferences before passing through a sample. This is converted from a time to a frequency domain using Fourier transformation to produce an IR spectrum [35]. A schematic of the instrument is displayed in Figure 2.6.



Figure 2.5 Thermo Nicolet iS50 FTIR Spectrometer

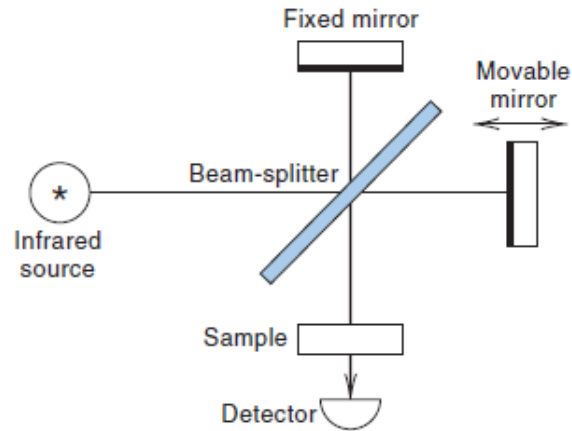


Figure 2.6 Schematic of an interferometer [33]

### **2.2.2 Indirect Tensile Test**

The Indirect Tensile (IDT) test method was primarily used for concrete until researchers began applying the technique for other materials after 1962. The IDT procedure was utilized to determine the low-temperature tensile properties of asphalt mixtures, standardized in AASHTO T322. IDT testing has been re-evaluated as a simple method for assessing both permanent deformation and fatigue cracking [36]. Christensen et. al. [37] conducted a test temperature representative of the critical pavement temperature and found the IDT to be an inexpensive and effective test for evaluating the rutting resistance of asphalt mixtures. The calculation of IDT strength according to ASTM D 6931 is as follows:

$$S_t = \frac{2000 \times P}{\pi \times t \times D}, \text{ where:}$$

$S_t$  = IDT strength, kPa

$P$  = maximum load, N

$t$  = specimen height before test, mm

$D$  = specimen diameter, mm

The test involves applying a static, compressive load on a horizontally placed cylindrical sample. This develops uniform tensile stress perpendicular to the applied load, depicted in Figure 2.7.

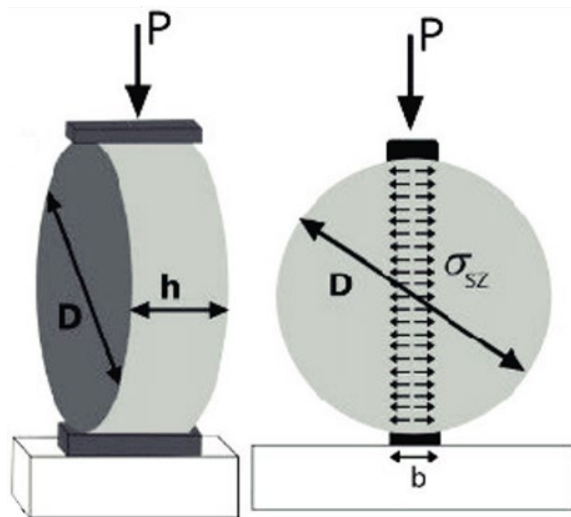


Figure 2.7 IDT sample schematic [38]

### 2.2.3 Scanning Electron Microscopy

Scanning electron microscopes (SEM), shown in Figure 2.8, are used to qualitatively and semi-quantitatively characterize solid materials. Using an electron

source, SEM has the ability to generate high-resolution images as elastic and inelastic interactions occur between electron beam and sample, illustrated in Figure 2.9. The produced signals include secondary electrons that produce SEM images, backscattered electrons (BSE), characteristic x-rays for Energy-Dispersive X-ray Spectroscopy (EDS), and other irradiation. The topography and composition of a specimen can be determined using the BSE mode whereas an EDS detector can further analyze the chemical composition to specific areas of interest [40].

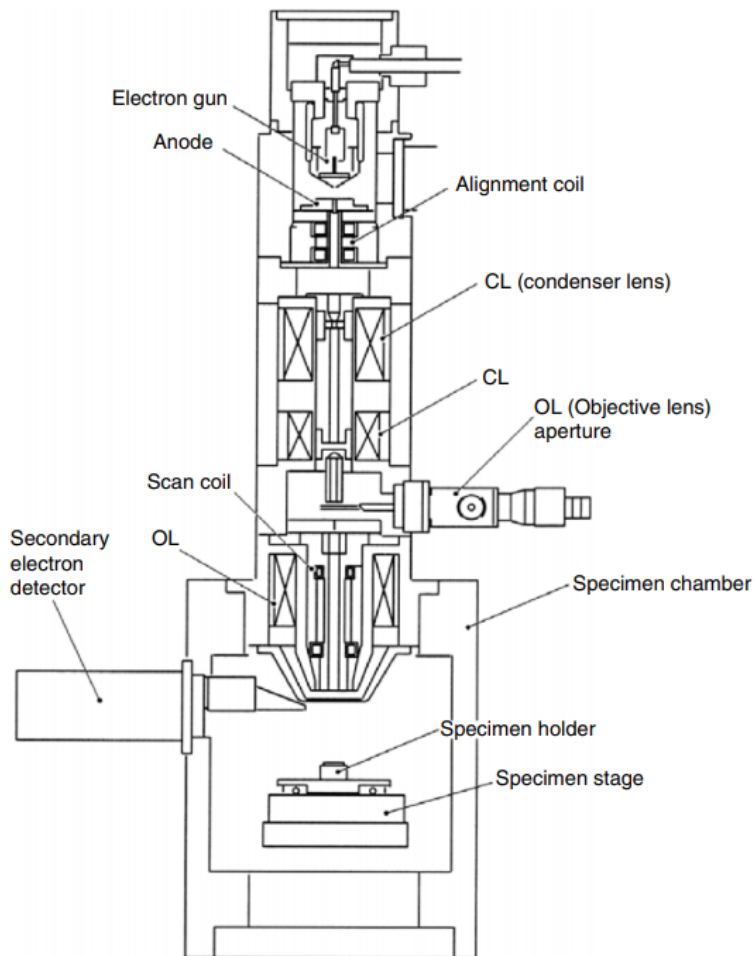


Figure 2.8 Schematic diagram of a SEM [39]

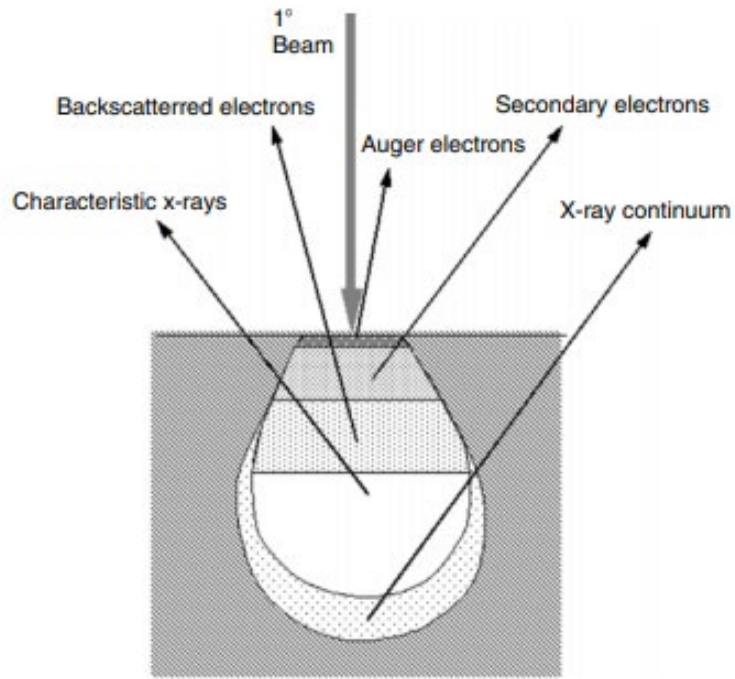


Figure 2.9 Illustration of signals generated from electron-specimen interactions [39]

## CHAPTER 3

### METHODOLOGY

#### 3.1 Experimental Procedure

In this study, the samples were formulated with PG 64-22 asphalt obtained from TexasBit, fine and coarse aggregate acquired from Cemex S.A.B., polyethylene from plastic bags, and organic montmorillonite nanoparticles purchased from Sigma-Aldrich. The properties of the nanoclay are shown in Table 3.1.

The fine aggregates used in this study was a dry siliceous natural sand calibrated to 0-2 mm, conforming to the standard of ASTM C 778. Graded crushed limestone was used as the coarse aggregates, with a minimum and maximum nominal size of 4 and 16 mm, respectively. A gradation curve of the fine and coarse aggregates according to the ASTM C 33 limits are shown in Figure 3.1.

The specimens were composed in these mixtures: AS/PE, AS/PE/NC (NC: as received), and AS/PE/NC-d (NC-d: dispersion).

Table 3.1 Properties of nanoclay particles (NC)

Loss on drying	$\leq 18\%$
Bulk density	600 – 1100 kg/m <sup>3</sup>
Average particle size	$\leq 25 \mu\text{m}$

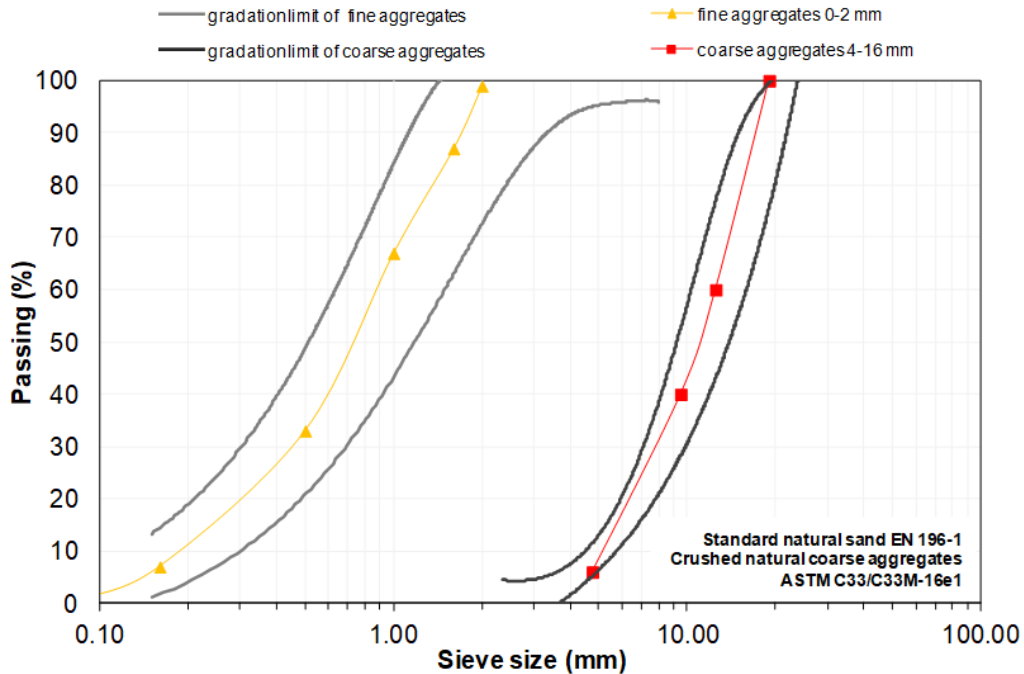


Figure 3.1 Graduation curves of fine and coarse aggregates

### 3.1.1 Dispersion of Nanoplatelets

The nanoplatelets were exfoliated prior to addition in the blend specimens. The NC were suspended in a solution containing 30 g of acetone and sonicated for 1 hour at a constant rate of 1000 J/min, set at 30% amplitude. The acetone was evaporated and the nanoclay dried in a vacuum chamber at 100 °C for 24 hours.

### 3.1.2 Preparation of Modified Asphalt Specimens

The quantities of the components were calculated to form cylindrical specimens with a height of 3.25 cm and a diameter of 7.5 cm, presented in Table 3.1. Following the shear mixing procedure described in AASHTO R 35 and TxDOT designation Tex-340. The waste polyethylene was cut into small pieces and added to molten asphalt with or



without the nanoclay. The blend was stirred at 180 °C for 2 hours at a constant rotational speed of 125 rpm using an intensive mixer, shown in Figure 3.2, to uniformly distribute the PE and NC in the asphalt. Subsequently, equal proportions of fine and coarse aggregates were added and combined on heat. The blends were compacted in cylindrical molds and set for 24 hours. The product is exhibited in Figure 3.3.

Table 3.2 Composition of modified asphalt specimens by weight percent

Specimen	Aggregates	PG 64-22 (AS)	Polyethylene (PE)	Nanoclay (NC)
AS	95.0	5.0	—	—
AS/PE	95.0	4.7	0.3	—
AS/NC-d	95.0	4.8	—	0.2
AS/PE/NC	95.5	4.0	0.3	0.2
AS/PE/NC-d				



Figure 3.2 EIRICH Intensive Mixer Type RV02E

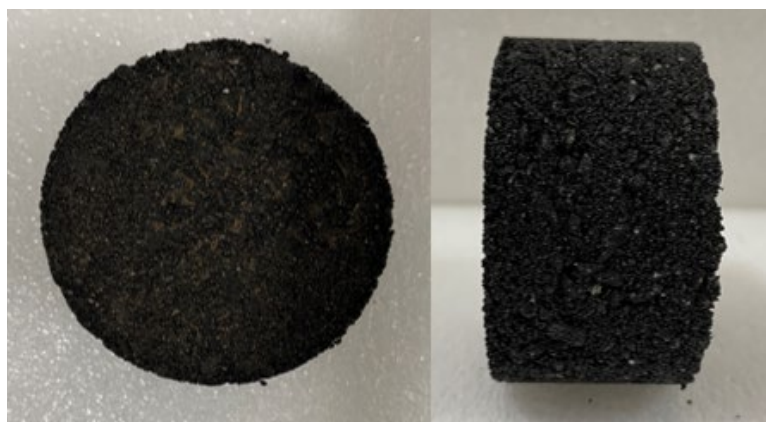


Figure 3.3 Top and side view of the AS/PE sample

### 3.2 FTIR Characterization

The individual materials and blend specimens were characterized using the Thermo Nicolet iS50 FTIR Spectrometer in the UTA Characterization Center for

Materials and Biology (CCMB). Using the OMNIC™ Software Suite, the analyses were executed with 32 scans at wavenumbers from 4000 to 525  $\text{cm}^{-1}$ .

### 3.3 IDT Testing

The stress-strain behavior of the specimens was evaluated using the MTS Criterion Model 43 in the UTA Center for Advanced Construction Materials (CACM). A sample assembled for testing is displayed in Figure 3.4. The IDT strength tests were conducted at 25 °C. Utilizing the MTS TestSuite™ TW Software, the load was applied at a rate of 2 in/min. The indirect tensile strengths were calculated in accordance with ASTM D 6931.

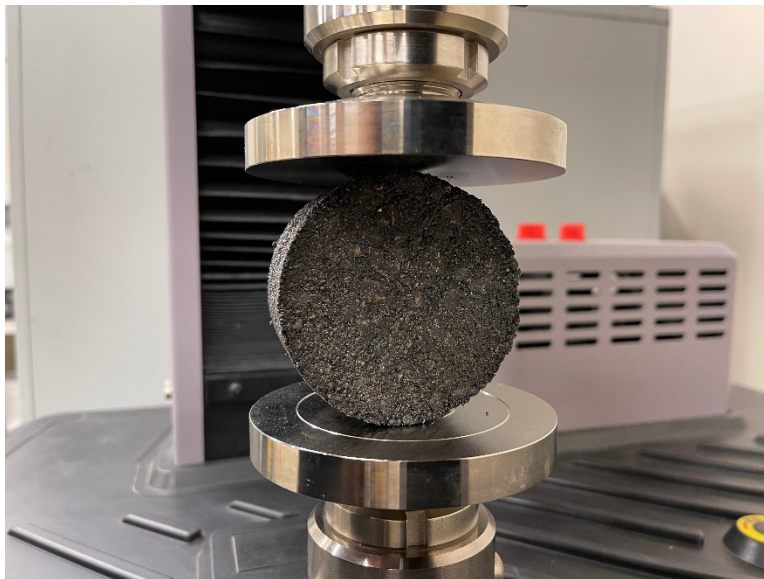


Figure 3.4 IDT strength test of the AS/PE sample

### 3.4 SEM Analysis

The AS/PE/NC-d specimen was analyzed using the HITACHI S-3000N SEM, photographed in Figure 3.5, in the CCMB. The sample was examined in BSE mode at low vacuum (20 Pa) with the accelerating voltage was set to 25.0 kV. Spot chemical analysis and elemental mapping were performed using EDS.

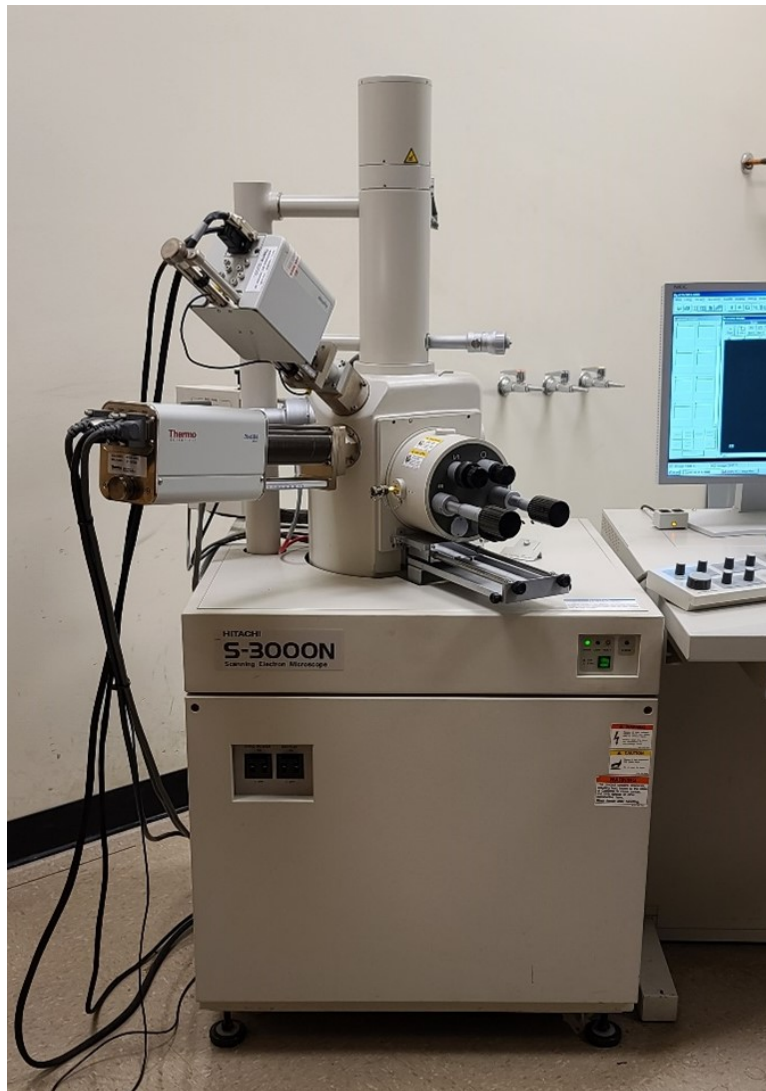


Figure 3.5 HITACHI S-3000N SEM

## CHAPTER 4

### RESULTS AND DISCUSSION

#### 4.1 FTIR Characterization

Each component of the blends was analyzed using FTIR spectroscopy to determine the chemical interactions between the components with the exception of the aggregates.

A comparison of the nanoclay before and after dispersion is shown in Figure 4.1. Both signals exhibit the same peaks with different intensities. The most prominent peak at  $955\text{ cm}^{-1}$  corresponds to the Si-O in-plane stretching vibrations from the nanoclay [41]. The -OH stretching and calcite bending are visible around  $3280\text{ cm}^{-1}$  and  $1517\text{ cm}^{-1}$  respectively. There are also signals for quartz vibrations and Al-O-Si, Al-OH bending in the fingerprint region [42]. The dispersed nanoclay exhibited a lower transmittance in contrast to the nanoclay as received. The lower transmittance can be interpreted as more Si-O bonds occurring due to the formation of individual silicate layers without hinderance of the octahedral sheet. The higher population of available Si-O bonds produces more vibrational energy as additional corresponding radiation is absorbed [43]. Erdmann et. al. [44] have observed similar results.

The asphalt and polyethylene have distinct features in their structure, allowing for easy identification as seen in Figure 4.2. The C-H stretching vibrations of the asphalt binder were confirmed at  $2848\text{ cm}^{-1}$  and  $2915\text{ cm}^{-1}$ . C-H bending vibrations are also observed at  $717\text{ cm}^{-1}$  and  $1471\text{ cm}^{-1}$  correspondingly [45]. Similarly, these peaks are also apparent for the polyethylene signal. C-C bending and stretching indicators were observed around  $800\text{-}900\text{ cm}^{-1}$  and  $1580\text{ cm}^{-1}$  respectively.

The analyses of the asphalt blends in Figure 4.3 yielded similar results to the literature spectra [41,46]. At  $1376\text{ cm}^{-1}$ , the C-H bending peak becomes more distinct for each of the specimens, inferring an increase of asphalt and polymer interactions. There were no significant shifts to the band positions of the C-H region that suggests changes to the asphalt or polymer structure in the blends. The emerging  $1064\text{ cm}^{-1}$  peak of the dispersed samples was indicative of a new Si-O non-bonding interactions between the components and nanoclay. This was attributed to the misorientation of the clay layers and intercalation within the matrix. This could potentially result in a better blended phased morphology of the specimen. These results demonstrate the effectiveness of ultrasonication for the dispersion/exfoliation of the nanoclay to improve the compatibility between the asphalt and polymer.

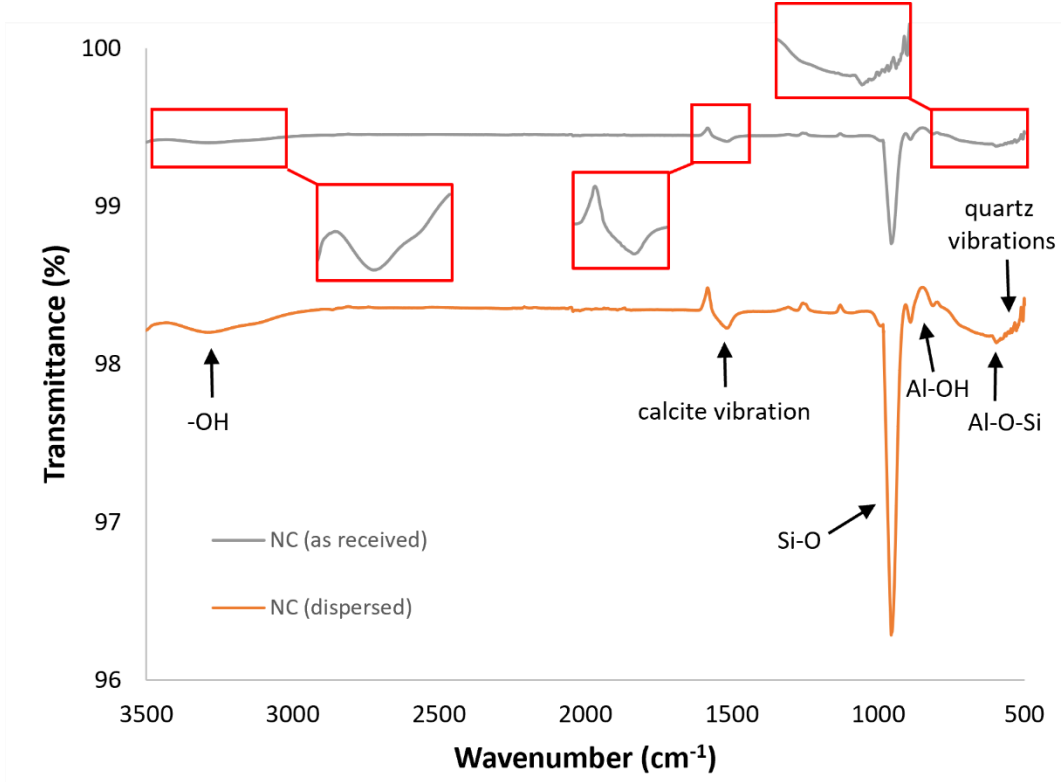


Figure 4.1 FTIR spectra of dispersed vs. non-dispersed nanoclay

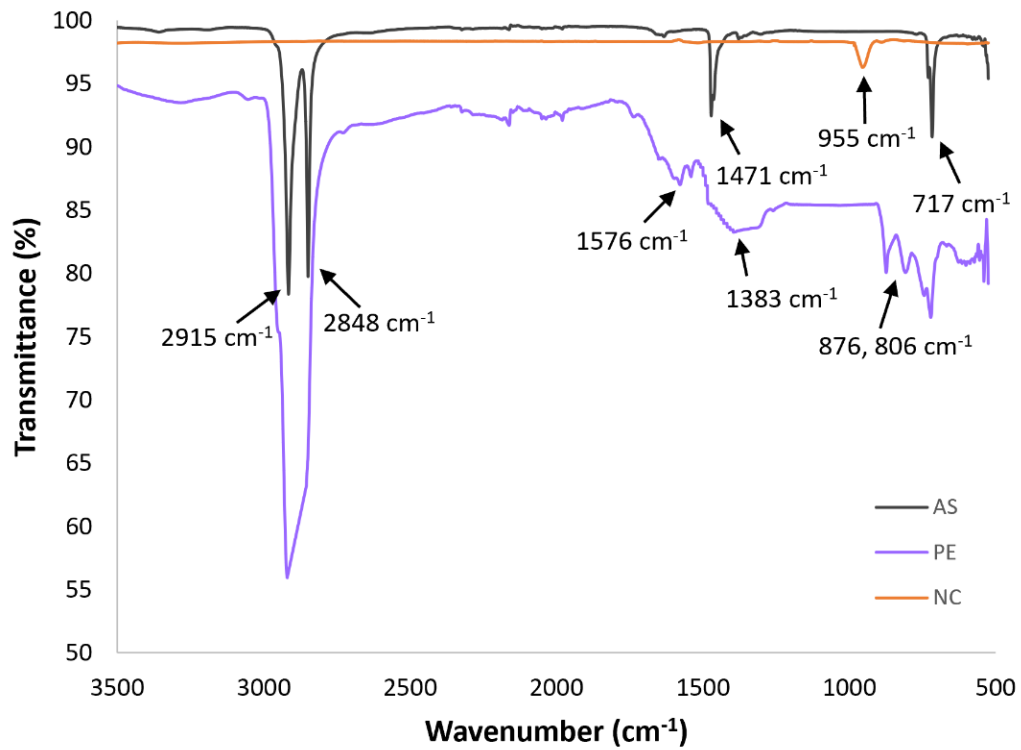


Figure 4.2 FTIR spectra of PG 64-22 asphalt, polyethylene, and nanoclay



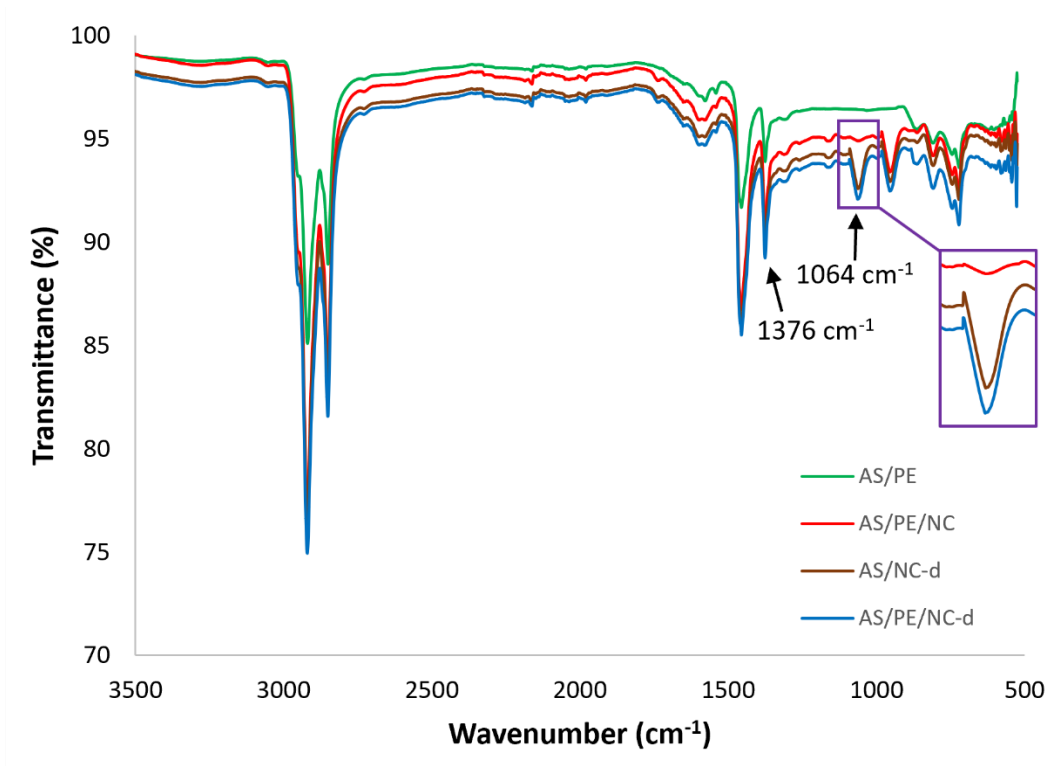


Figure 4.3 FTIR spectra of asphalt blends

## 4.2 Stress-Strain Behavior of Asphalt Blends

The stress-strain curves of the specimens show a clear trend in the development of asphalt strength, shown in Figure 4.4. Each progression showed an increase of indirect tensile strength, calculated in Table 4.1. When modifying asphalt with the plastic and dispersed nanoclay individually, both samples proved beneficial to the strength. So, the combination of all three parts should display further enhancement.

Compared to the base asphalt specimen, AS/PE/NC-d resulted in a 40% increase in tensile strength. This is three times the improvement of the AS/PE/NC specimen without prior dispersion of the nanoclay. The synergy between the components was improved with dispersion as shown with the enhancement of the tensile strength.

This data also suggested a higher modulus of elasticity as demonstrated with the greater stress-strain ratio of the exfoliated blend. Therefore, the proposed product has an enhanced resistance to cracking at lower temperatures. Although further testing of viscoelastic properties and temperature dependence are needed, there are indications of increased fatigue cracking resistance as well.

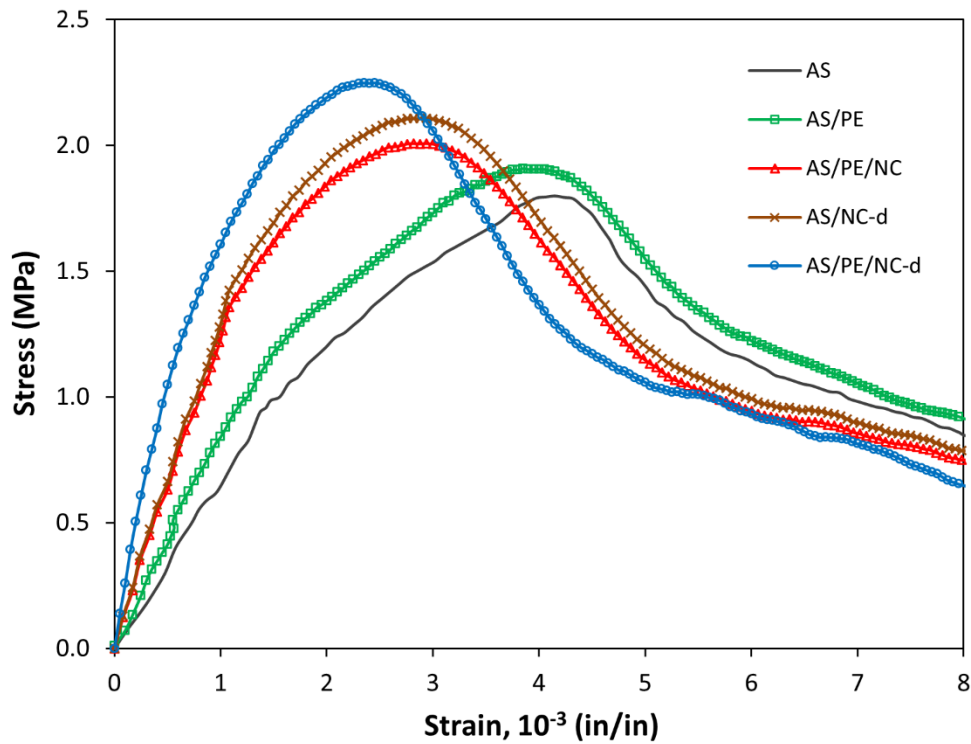


Figure 4.4 Stress-strain curve of IDT testing of the specimens

Table 4.1 Indirect tensile strength of the specimens

	AS	AS/PE	AS/PE/NC	AS/NC-d	AS/PE/NC-d
$S_t$ (MPa)	1.79	1.91	2.01	2.20	2.50
$S_t$ increase (%)	—	6.7	12.3	22.3	39.7

### 4.3 Fracture Surface Imaging

The fracture surface of the AS/PE/NC-d sample was examined using BSE mode on the SEM. Images were taken at two different magnifications, 450x and 1800x, shown in Figures 4.5 and 4.6. The former image displayed a broad view of the sample surface with heavier elements indicated as brighter areas. The dimmer areas appear to be the AS/PE adhering to the lighter aggregates.

The latter image contained more distinguishable components. Using EDS, spot chemical analysis was performed with the spectra portrayed in Figure 4.7. The significant element peaks are summarized as atomic percentage in Table 4.2. Spot 1 was determined to be a NC particle as Si, O, and Al were the predominant peaks. The particle size was also as expected. For spot 2, the component was concluded to be the aggregates composed of limestone ( $\text{CaCO}_3$ ). Spot 3 is assumed to be asphalt with the atom percent comparison of C and S. The composition values agree with the literature [47]. These findings were also confirmed with elemental composition mapping illustrated in Figure 4.8. The polymer was not well represented as hydrogen cannot be detected and the C atoms could be attributed to the asphalt or aggregate. However, the

interfaces between the components could be ascertained with different imaging mode analyses.

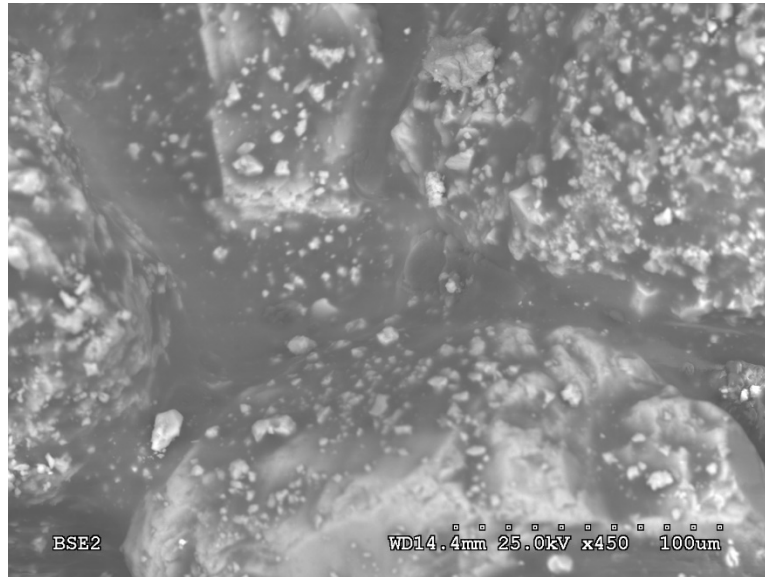


Figure 4.5 BSE-SEM image of AS/PE/NC-d at 450x magnification

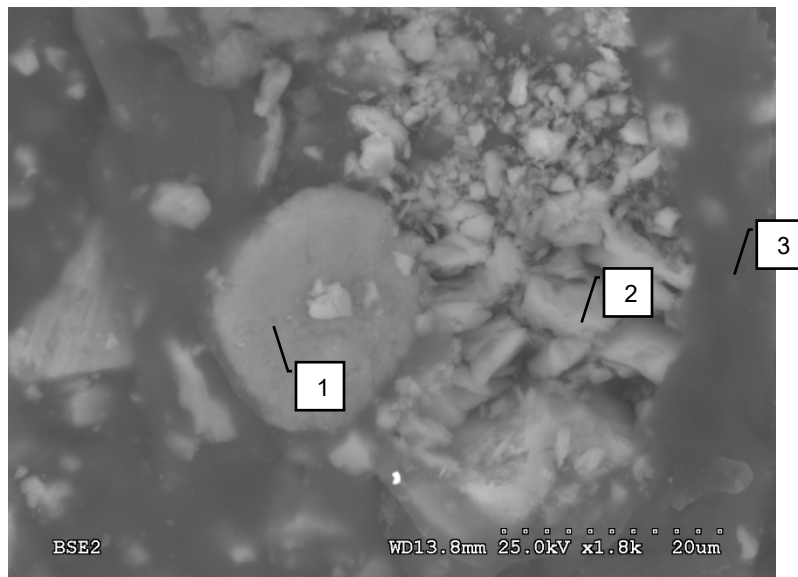


Figure 4.6 BSE-SEM image of AS/PE/NC-d at 1800x magnification

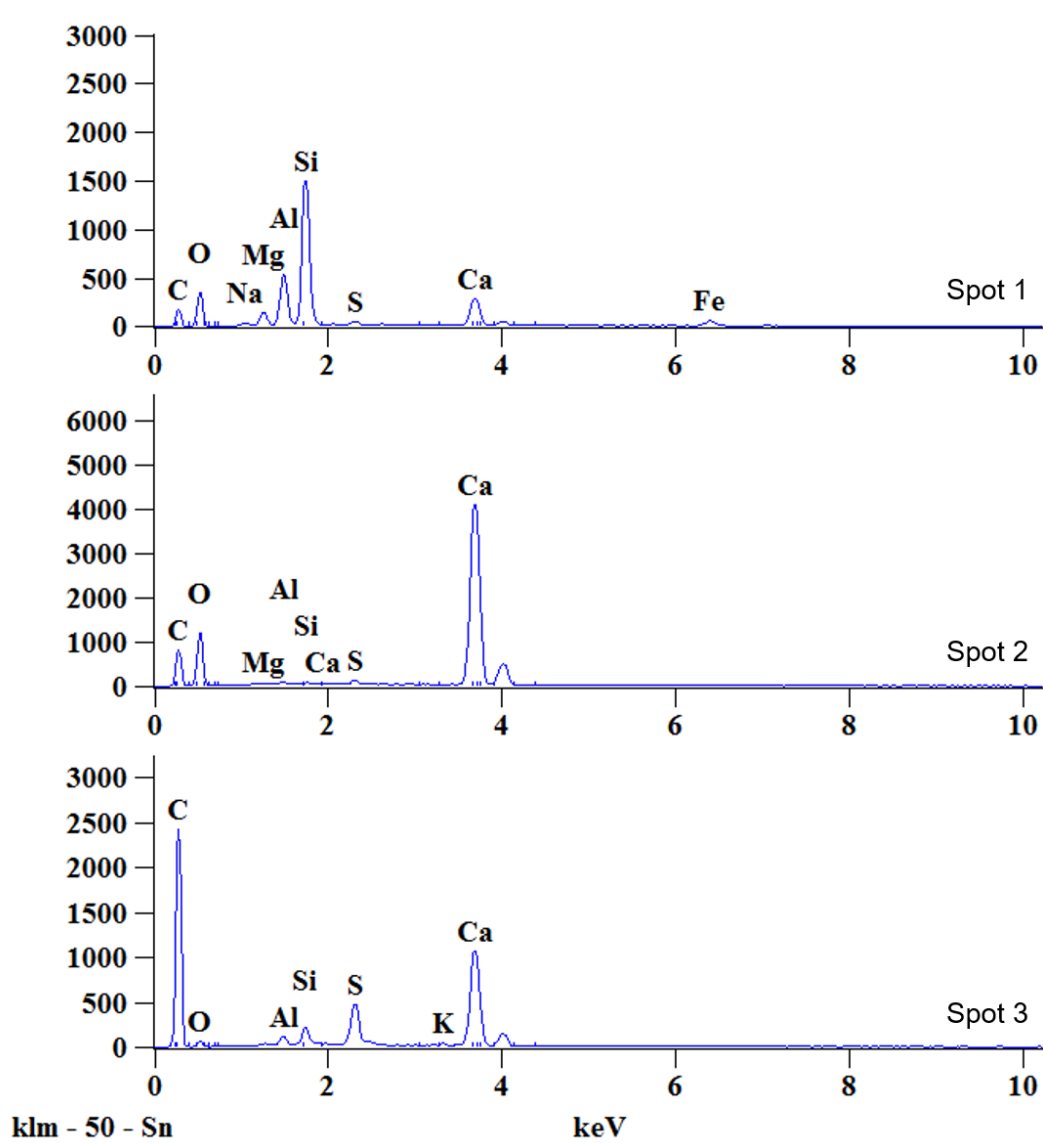


Figure 4.7 EDS spectra of spot analyses

Table 4.2 Atom percent of spots at 1800x magnification

Spot	C	Ca	O	Si	Al	S
1	30.2	5.5	30.4	22.2	6.7	0.9
2	24.7	35.0	39.0	0.2	0.4	0.4
3	84.7	9.7	1.1	0.8	0.5	3.2

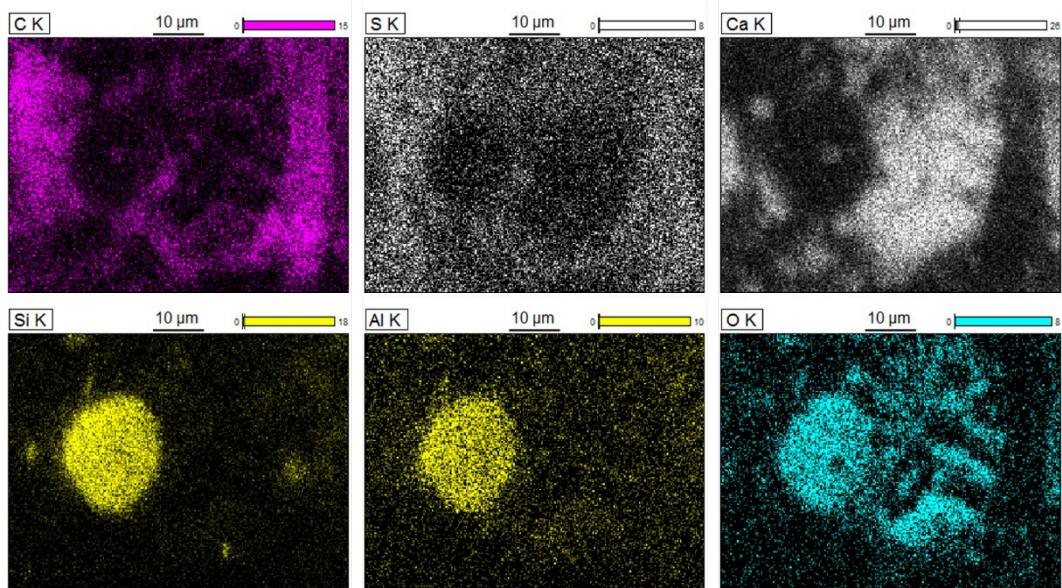


Figure 4.8 Element composition mapping at 1800x magnification

## CHAPTER 5

### CONCLUSIONS AND FUTURE RESEARCH

#### 5.1 Conclusions

This study represents preliminary research of a novel technique incorporating dispersed organic montmorillonite nanoplatelets in asphalt-plastic blends. The comparison of plain asphalt concrete specimens with modifications of polyethylene and dispersed/non-dispersed nanoclay were investigated.

FTIR analysis suggests that there is a new chemical interaction between the exfoliated NC and modified asphalt. A better-blended phase morphology is also suggested for the dispersed specimen. IDT strength testing shows a 40% increase of tensile strength in the dispersed NC blends compared to the base asphalt. This was significantly higher than the blends without NC or dispersion. A higher stress-strain ratio for the AS/PE/NC-d blend that indicates a greater elastic modulus than the other blends. SEM imaging of the fracture surface identified the dispersed NC in the AS/PE/NC-d matrix.

In conclusion, the method of ultrasonication for dispersion/exfoliation of nanoclay is an effective technique in enhancing the mechanical performance of the modified asphalt pavements.

#### 5.2 Future research

The recommendations for future research include studies of common waste plastics such as low and high-density polyethylene, polyethylene terephthalate, and polyvinyl chloride. Another asphalt binder used in Texas, PG 64-28, is intended to be

included in upcoming research. The combination with the asphalt performance grades and component ratios will also be considered.

Additional characterization studies of the interfaces of the different blends will be conducted. Optimization experiments are planned regarding the dispersion state and mechanical properties for the determinations of the highest increases of thermal stability and mechanical performance. Lastly, large-scale demonstrations and long-term studies should be done to validate the serviceability of the prototype.

The completion of this project will bring further advance highway engineering not only in the United States, but around the world, with benefits to the environment.



## REFERENCES

- [1] Fang, C., Wu, C., Hu, J., Yu, R., Zhang, Z., Nie, L., Zhou, S., Mi, X. (2014). Pavement properties of asphalt modified with packaging-waste polyethylene. *Journal of Vinyl and Additive Technology*, 20(1), 31–35. <https://doi.org/10.1002/vnl.21328>
- [2] Zhang, F., & Hu, C. (2015). The research for crumb rubber/waste plastic compound modified asphalt. *Journal of Thermal Analysis and Calorimetry*, 124(2), 729–741. <https://doi.org/10.1007/s10973-015-5198-4>
- [3] Modarres, A., & Hamed, H. (2014). Effect of waste plastic bottles on the stiffness and fatigue properties of modified asphalt mixes. *Materials & Design*, 61, 8–15. <https://doi.org/10.1016/j.matdes.2014.04.046>
- [4] Wu, S., & Montalvo, L. (2021). Repurposing waste plastics into cleaner asphalt pavement materials: A critical literature review. *Journal of Cleaner Production*, 280, 124355. <https://doi.org/10.1016/j.jclepro.2020.124355>
- [5] Poulidakos, L. D., Papadaskalopoulou, C., Hofko, B., Gschösser, F., Cannone Falchetto, A., Bueno, M., Arraigada, M., Sousa, J., Ruiz, R., Petit, C., Loizidou, M., Partl, M. N. (2017). Harvesting the unexplored potential of European waste materials for road construction. *Resources, Conservation and Recycling*, 116, 32–44. <https://doi.org/10.1016/j.resconrec.2016.09.008>
- [6] Vasudevan, R., Ramalinga Chandra Sekar, A., Sundarakannan, B., & Velkennedy, R. (2012). A technique to dispose waste plastics in an ecofriendly way – Application in construction of flexible pavements. *Construction and Building Materials*, 28(1), 311–320. <https://doi.org/10.1016/j.conbuildmat.2011.08.031>

- [7] *Trial recycles plastic containers into asphalt*. Fulton Hogan. (2018, April 4). <https://www.fultonhogan.com/trial-recycles-plastic-containers-asphalt/>.
- [8] *Recycled plastic milk bottles used to repave roads in South Africa*. Springwise. (2019, December 30). <https://www.springwise.com/sustainability-innovation/property-construction/shisalanga-construction-recycled-plastic-bottles-roads-south-africa>.
- [9] Stevenson, J. (2021). *Pavement Manual*: Texas Department of Transportation.
- [10] Norouzi, A., Kim, D., & Kim, Y. R. (2015). Numerical evaluation of pavement design parameters for the fatigue cracking and rutting performance of asphalt pavements. *Materials and Structures*, 49(9), 3619–3634. <https://doi.org/10.1617/s11527-015-0744-x>
- [11] Zou, G., Xu, J., & Wu, C. (2017). Evaluation of factors that affect rutting resistance of asphalt mixes by orthogonal experiment design. *International Journal of Pavement Research and Technology*, 10(3), 282–288. <https://doi.org/10.1016/j.ijprt.2017.03.008>
- [12] *Fatigue Cracking*. Pavement Interactive. (2018, September 21). <https://pavementinteractive.org/reference-desk/pavement-management/pavement-distresses/fatigue-cracking/>.
- [13] Shi, C. & Guo, Z. (2008). Mechanical properties of asphalt pavement structure in highway tunnel. *Journal of Shanghai Jiaotong University (Science)*, 13(2), 206–210. <https://doi.org/10.1007/s12204-008-0206-5>
- [14] Liley, C. (2018). *Rutting: Causes, Preventions, and Repairs*: Illinios Asphalt Pavement Association.

- [15] *Rutting*. Pavement Interactive. (2018, September 20).  
<https://pavementinteractive.org/reference-desk/pavement-management/pavement-distresses/rutting/>.
- [16] Petersen, J.C., (1984) *Chemical Composition of Asphalt as Related to Asphalt Durability: State of the Art*. Transportation Research Board 999, 13-30.
- [17] Al-Taher, M., Mohamady, A., Shalaby, M.A. (2008) Evaluation of asphalt Pavements Constructed using Novophalt. *Emirates Journal for Engineering Research*. 13(1), 13-20.
- [18] Costa, L., Fernandes, S., Silva, H., & Oliveira, J. (2017). Study of the interaction between asphalt and recycled plastics in new polymer modified binders (PMB). *Ciência & Tecnologia Dos Materiais*, 29(1).  
<https://doi.org/10.1016/j.ctmat.2016.04.005>
- [19] Sojobi, A. O., Nwobodo, S. E., & Aladegboye, O. J. (2016). Recycling of polyethylene terephthalate (PET) plastic bottle wastes in bituminous asphaltic concrete. *Cogent Engineering*, 3(1), 1133480.  
<https://doi.org/10.1080/23311916.2015.1133480>
- [20] Wen, G., Zhang, Y., Zhang, Y., Sun, K., & Chen, Z. (2001). Vulcanization characteristics of asphalt/sbs blends in the presence of sulfur. *Journal of Applied Polymer Science*, 82(4), 989-996. doi:10.1002/app.1932
- [21] Wu, S., Pang, L., Mo, L., Chen, Y., & Zhu, G. (2009). Influence of aging on the evolution of structure, morphology and rheology of base and sbs modified bitumen. *Construction and Building Materials*, 23(2), 1005-1010.  
doi:10.1016/j.conbuildmat.2008.05.004

- [22] Fu, Z., Jia, J., Li, J., & Liu, C. (2017). Transforming waste expanded polystyrene foam into hyper-crosslinked polymers for carbon dioxide capture and separation. *Chemical Engineering Journal*, 323, 557-564. doi:10.1016/j.cej.2017.04.090
- [23] Leng, Z., Sreeram, A., Padhan, R. K., & Tan, Z. (2018). Value-added application of waste pet based additives in bituminous mixtures containing high percentage of reclaimed asphalt pavement (rap). *Journal of Cleaner Production*, 196, 615-625. doi:10.1016/j.jclepro.2018.06.119
- [24] Bala, N., Napiah, M., & Kamaruddin, I. (2018). Effect of nanosilica particles on polypropylene polymer modified asphalt mixture performance. *Case Studies in Construction Materials*, 8, 447-454. doi:10.1016/j.cscm.2018.03.011
- [25] Mansourian, A., Goahri, A. R., & Khosrowshahi, F. K. (2019). Performance evaluation of ASPHALT binder modified with eva/hdpe/nanoclay based on linear and NON-LINEAR viscoelastic behaviors. *Construction and Building Materials*, 208, 554-563. doi:10.1016/j.conbuildmat.2019.03.065
- [26] You, Z., Mills-Beale, J., Foley, J. M., Roy, S., Odegard, G. M., Dai, Q., & Goh, S. W. (2011). Nanoclay-modified asphalt materials: Preparation and characterization. *Construction and Building Materials*, 25(2), 1072–1078. <https://doi.org/10.1016/j.conbuildmat.2010.06.070>
- [27] Venkatesha, N. J. (2015). *Pore architecture modulated clays and zeolites as solid acid catalysts for selected organic reactions* [Doctoral dissertation, Visvesvaraya Technological University]. ResearchGate.

- [28] Zhu, T. T., Zhou, C. H., Kabwe, F. B., Wu, Q. Q., Li, C. S., & Zhang, J. R. (2019). Exfoliation of montmorillonite and related properties of clay/polymer nanocomposites. *Applied Clay Science*, 169, 48–66.  
<https://doi.org/10.1016/j.clay.2018.12.006>
- [29] Fang, C., Yu, R., Zhang, Y., Hu, J., Zhang, M., & Mi, X. (2012). Combined modification of asphalt with polyethylene packaging waste and organophilic montmorillonite. *Polymer Testing*, 31(2), 276-281.  
<https://doi.org/10.1016/j.polymertesting.2011.11.008>
- [30] Yu, J., Zeng, X., Wu, S., Wang, L., & Liu, G. (2007). Preparation and properties of montmorillonite modified asphalts. *Materials Science and Engineering: A*, 447(1-2), 233–238. <https://doi.org/10.1016/j.msea.2006.10.037>
- [31] Daniel, I. M., Miyagawa, H., Gdoutos, E. E., & Luo, J. J. (2003). Processing and characterization of epoxy/clay nanocomposites. *Experimental Mechanics*, 43(3), 348–354. <https://doi.org/10.1007/bf02410534>
- [32] Du, Z., Jiang, C., Yuan, J., Xiao, F., & Wang, J. (2020). Low temperature performance characteristics of polyethylene modified asphalts – A review. *Construction and Building Materials*, 264, 120704.  
<https://doi.org/10.1016/j.conbuildmat.2020.120704>
- [33] Christian, G. D., Dasgupta, P. K., & Schug, K. A. (2014). Chapter 16 Spectrochemical Methods. In *Analytical chemistry*. essay, J. Wiley & Sons.
- [34] Thermo Scientific. (2013). *Introduction to Fourier Transform Infrared Spectroscopy*.

- [35] Silverstein, R. M., Webster, F. X., & Kiemle, D. J. (2005). Chapter 2 Infrared Spectrometry. In *Spectrometric identification of organic compounds*. essay, John Wiley & Sons.
- [36] Bennert, T., Haas, E., & Wass, E. (2018). Indirect Tensile Test (IDT) to Determine Asphalt Mixture Performance Indicators during Quality Control Testing in New Jersey. *Transportation Research Record: Journal of the Transportation Research Board*, 2672(28), 394–403. <https://doi.org/10.1177/0361198118793276>
- [37] Christensen, D. W., Bonaquist, R., Anderson, D. A., & Gokhale, S. (2004) Indirect Tension Strength as a Simple Performance Test. New Simple Performance Tests for Asphalt Mixtures. *Transportation Research Circular, E-C068*, 44–57.
- [38] Kavussi, A., Hassani, A., Kazemian, F., & Taghipoor, M. (2019). Laboratory evaluation of treated recycled concrete aggregate in asphalt mixtures. *International Journal of Pavement Research and Technology*, 12(1), 26–32. <https://doi.org/10.1007/s42947-019-0004-5>
- [39] Zhou W., Apkarian R., Wang Z.L., Joy D. (2006) Fundamentals of Scanning Electron Microscopy (SEM). In: Zhou W., Wang Z.L. (eds) *Scanning Microscopy for Nanotechnology*. Springer, New York, NY. [https://doi.org/10.1007/978-0-387-39620-0\\_1](https://doi.org/10.1007/978-0-387-39620-0_1)
- [40] *Scanning Electron Microscopy (SEM)*. Techniques. (2017, May 26). [https://serc.carleton.edu/research\\_education/geochemsheets/techniques/SEM.html](https://serc.carleton.edu/research_education/geochemsheets/techniques/SEM.html)

- [41] Sikdar, D., Katti, K. S., & Katti, D. R. (2008). Molecular Interactions Alter Clay and Polymer Structure in Polymer Clay Nanocomposites. *Journal of Nanoscience and Nanotechnology*, 8(4), 1638–1657. <https://doi.org/10.1166/jnn.2008.18228>
- [42] Caccamo, M. T., Mavilia, G., Mavilia, L., Lombardo, D., & Magazù, S. (2020). Self-Assembly Processes in Hydrated Montmorillonite by FTIR Investigations. *Materials*, 13(5), 1100. <https://doi.org/10.3390/ma13051100>
- [43] Libretexts. (2020, August 21). *IR Spectroscopy Background*. Chemistry LibreTexts. [https://chem.libretexts.org/Bookshelves/Physical\\_and\\_Theoretical\\_Chemistry\\_Textbook\\_Maps/Supplemental\\_Modules\\_\(Physical\\_and\\_Theoretical\\_Chemistry\)/Spectroscopy/Vibrational\\_Spectroscopy/Infrared\\_Spectroscopy/IR\\_Spectroscopy\\_Background](https://chem.libretexts.org/Bookshelves/Physical_and_Theoretical_Chemistry_Textbook_Maps/Supplemental_Modules_(Physical_and_Theoretical_Chemistry)/Spectroscopy/Vibrational_Spectroscopy/Infrared_Spectroscopy/IR_Spectroscopy_Background).
- [44] Erdmann, E., Acosta, D., Pita, V. J., Monasterio, F. E., Carrera, M. C., Dias, M. L., & Destéfánis, H. A. (2010). Effect of the organoclay preparation on the extent of intercalation/exfoliation and barrier properties of polyethylene/PA6/montmorillonite nanocomposites. *Journal of Applied Polymer Science*. <https://doi.org/10.1002/app.32560>
- [45] Xiao, F., Punith, V. S., & Amirkhanian, S. N. (2012). Effects of non-foaming WMA additives on asphalt binders at high performance temperatures. *Fuel*, 94, 144–155. <https://doi.org/10.1016/j.fuel.2011.09.017>
- [46] Abdelrahman, M., Katti, D. R., Ghavibazoo, A., Upadhyay, H. B., & Katti, K. S. (2014). Engineering Physical Properties of Asphalt Binders through Nanoclay–Asphalt Interactions. *Journal of Materials in Civil Engineering*, 26(12), 04014099. [https://doi.org/10.1061/\(asce\)mt.1943-5533.0001017](https://doi.org/10.1061/(asce)mt.1943-5533.0001017)

[47] Petersen, J. C. (2000). Chapter 14 Chemical Composition of Asphalt as Related to Asphalt Durability. *Developments in Petroleum Science*, 363–399.

[https://doi.org/10.1016/s0376-7361\(09\)70285-7](https://doi.org/10.1016/s0376-7361(09)70285-7)